Available online at www.sciencedirect.com

ScienceDirect

IFAC Papers Online CONFERENCE PAPER ARCHIVE

IFAC PapersOnLine 51-20 (2018) 307–312

Potential-field constructions in an MPC framework: application for safe navigation in a variable coastal environment

N.Q.H. Tran * **I. Prodan** * **E. I. Grøtli** ** **L. Lefèvre** *

* *Univ. Grenoble Alpes, Grenoble INP, LCIS, F-26000, Valence, France (ngo-quoc-huy.tran, ionela.prodan, laurent.lefevre@lcis.grenoble-inp.fr).*

** *Mathematics and Cybernetics, SINTEF Digital, Norway (Esten Ingar.Grotli@sintef.no).*

Abstract: This work presents an NMPC (Nonlinear Model Predictive Control)-based algorithm for safe navigation of multi-agent dynamical systems in a variable environment with fixed or moving obstacles. The contribution lies in the construction of repulsive potential fields for the fixed and moving obstacles which are introduced in a predictive control optimization problem to penalize collision. The constraints are activated only in the view range of the agent using on-off barrier functions. Collision-free motion planning of ships in Trondheim fjord harbor serves as a benchmark for testing our algorithm. Some scenarios are simulated in order to prove the efficiency of the algorithm and its feasibility to run in real-time.

Keywords: Fixed/Moving obstacles avoidance, NMPC (Nonlinear Model Predictive Control), Potential field constructions, On-off barrier functions, ASV (Autonomous surface vehicles).

1 INTRODUCTION

Autonomous systems, often included under the paradigm of multi-agent dynamical systems, are proving to be worthwhile in places where man cannot reach or is unable to perform in a timely and efficient manner. In particular, for autonomous marine vehicles it is important to generate collision-free paths with fixed obstacles (e.g., islands, shorelines or ships anchoring) or moving obstacles (e.g., another ships are operating). The collision avoidance actions for both manned and unmanned surface vessels must respect the rules which have been given by the International Regulations for Preventing Collisions at Sea (COLREGS) (Commandant, 1999).

From a control point of view, we may classify the methods which tackle the collision avoidance problem with fixed/moving obstacles in explicit and implicit methods. Usually the explicit methods reduce to the use of MIP (Mixed-Integer Programming) where the constraints are explicitly taken into account but with the cost of high computation time (Prodan et al., 2015). Moreover, when using the nonlinear vehicle dynamics, nonlinear mixed-integer optimization programs need to be solved (Abichandani et al., 2015). The implicit methods usually reduce to the use of various types of potential field-based constructions which prove to be efficient in many real applications (Rasekhipour et al., 2017). Furthermore, for the particular case of motion planning with collision avoidance at sea several methods are employed: i) use sensor data providing sub-optimal solutions with low computation demand (Dunbabin and Lament, 2017) or ii) build a 2D (two-dimentional) obstacle map from a priori information, each obstacle being represented by a cell-location in which the agent cannot enter (Song et al., 2017). Various works using these types of algorithms can be enumerated: some use collision cone concept (Chakravarthy and Ghose, 2012), velocity obstacles (Lee et al., 2017), artificial potential field (Tran et al., 2017), evolutionary method (Shin et al., 2017), MPC-based approaches using nonlinear programming (Breivik et al., 2017).

This paper proposes a collision avoidance algorithm via a coherent combination between potential field-based constructions and NMPC. It is applied over a benchmark using real numerical data for the safe navigation of ships in Trondheim fjord complying to COLREGS rules. More specifically the contributions of this paper are:

(1) construction of on-off barrier functions which activate the associated repulsive potential for fixed and moving obstacles;
(2) development of an NMPC-based algorithm which activates the constraints in the view range of the agent;
(3) validation of the proposed algorithm through simulations over a real benchmark of safe navigation of ships in the Trondheim fjord.

The paper is organized as follows. Section 2 formulates the problem and introduces the repulsive potential constructions. Section 3 introduces the construction of on-off barrier functions in conjunction with repulsive potential. After that, all the elements presented are gathered into a nonlinear model predictive control framework for motion planning with collision avoidance. Section 4 shows the simulation results over a real benchmark. Section 5 draws the conclusions and presents the future work.

2405-8963
Peer review under responsibility of International Federation of Automatic Control.
10.1016/j.ifacol.2018.11.049

2 PRELIMINARIES

This paper is inspired by the practical application of collision-free motion planning of unmanned surface vessels in the Trondheim fjord harbor, Norway. Fig. 1 illustrates the operating region of the ships which need to navigate from three different harbors (Orkanger, Stjørdal and Skogn) to Trondheim harbor while avoiding the shore or small islands and other ships (moving obstacles). The COLREGS rules [1] we consider hereafter are:

- Rule 8 - Action to avoid collision: avoidance action must be applied timely, before other vessel approaches. Any alterations of course and/or speed must be large enough to clear the approaching vessels.
- Rule 14 - Head on situation: when two power-driven vessels are meeting on nearly reciprocal courses so as to involve risk of collision, then alter course to starboard so that each pass on the port side of each other.
- Rule 15 - Crossing situation: when two power-driven vessels are crossing so as to involve risk of collision, the vessel which has the other on her own starboard side shall keep out of the way.
- Rule 16 - Actions by give-way vessel: take early and substantial action to keep well clear.

The Automatic Identification Systems (AIS) provided real numerical data related to position, velocity of ships, time of navigation between harbors.

In order to efficiently describe the non-convex feasible region for the dynamical (mobile) agent, we briefly recall here the system dynamics and various notions which involve polyhedral/ellipsoidal sets and repulsive potential constructions.

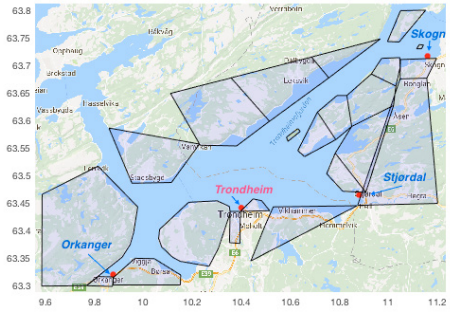

Fig. 1. Map of Trodheim obtained from real data: feasible space and considered forbidden cells as in (2).

The following notation will be used throughout the paper. For a vector $x \in \mathbb{R}^n$ and a positive definite matrix $P \in \mathbb{R}^{n\times n}$, $||x||_P$ denotes the weighted norm $\sqrt{x^T P x}$, $||x||$ the Euclidean norm and $|x|$ the absolute value of the vector x or an array x. We denote by $\|\Delta p_i\|$, $i = 1...N_{\text{cell}}$, the Euclidean distance calculated from Chebyshev center, the largest inscribed ball of i^{th} polytope and current position of an Autonomous Surface Vehicle (ASV). Similarly, $\|\Delta p_j\|$, $j = 1...N_{\text{mov}}$ is the Euclidean distance calculated from current position of an agent and j^{th} moving obstacle. The safe distance between the agent and a forbidden cell i is denoted by D_s^i. Also, ρ_{view} denotes the view range of the agent. A polytope is a bounded polyhedron and has a dual representation in terms of intersection of half-spaces or convex hull of extreme points: $\mathcal{P} = \{x \in \mathbb{R}^n : Sx \leq K\} = \{x \in \mathbb{R}^n : x = \sum \alpha_i v_i, \sum \alpha_i = 1, \alpha_i \geq 0\}$. An ellipsoid is denoted by $\mathcal{E}(c, W, r) = \{x \in \mathbb{R}^n : (x-c)^T W (x-c) \leq r^2\}$, with $W = W^T \succ 0$ and $r > 0$.

[1] http://astat.autonomous-ship.org/

2.1 Model Description

A classical model of an ASV (Pavlov et al., 2009) is used:

$$\begin{cases} \dot{\eta} = R(\psi)\nu, \\ M\dot{\nu} + C(\nu)\nu + D\nu = B\mathbf{u}. \end{cases} \tag{1}$$

where the state vector, $\mathbf{x} \in \mathbb{R}^6$, with $x = [\eta\ \nu]^\top$ includes the vector $\eta \in \mathbb{R}^3$, with $\eta = [x\ y\ \psi]^\top$ containing the system position and the yaw angle, ψ, in the inertial frame. The vector, $\nu \in \mathbb{R}^3$, with $\nu = [u\ v\ r]^\top$ is surge, sway and yaw rate. The input vector, $\mathbf{u} \in \mathbb{R}^2$, with $\mathbf{u} = [\tau_u\ \tau_r]^\top$ is the control input corresponding to surge thrust and rudder deflection. Also, in (1) $B \in \mathbb{R}^{3\times 2}$ is the actuator configuration matrix, $R(\psi)$, M, $C(\nu)$ and $D \in \mathbb{R}^{3\times 3}$ are the rotation, mass, Coriolis and damping matrices, respectively.

2.2 Repulsive potential for the fixed obstacles

Let us define the collection of forbidden cells (as also illustrated in Fig. 1) as a union of bounded polyhedral given by their half-space description:

$$\mathbb{P} = \bigcup_{i=1}^{N_{\text{cell}}} \mathcal{P}_i. \tag{2}$$

where $\mathcal{P}_i = \{x \in \mathbb{R}^n : a_k x \leq b_k, k = 1, ..., n_h\}$, $a_k \in \mathbb{R}^{1\times n}$, $b_k \in \mathbb{R}$, n_h and N_{cell} are the number of half-spaces and forbidden cells respectively.

Next, for the bounded convex set $\mathcal{P}_i$ we define the piecewise linear function (Camacho and Bordons, 2004):

$$\theta(x) = \sum_{k=1}^{n_h} (a_k(x - x_s) - b_k + a_k x_s + \mid a_k(x - x_s) - b_k + a_k x_s \mid) \tag{3}$$

with $x_s \in \mathbb{R}^n$ the analytic center [2] of the polytope $\mathcal{P}_i$. The function (3) is zero in the interior of the convex set $\mathcal{P}_i$ (2) and a non-zero value which grows linearly as the distance from convex region increases. $\theta(x)$ will be used for the construction of repulsive potential which takes into account the shape of the fixed obstacles (2).

Considering (3) we define the collection of repulsive potentials of the forbidden cells in (4) as:

$$\mathbb{V} = \bigcup_{i=1}^{N_{\text{cell}}} V_i^{\text{fix}}(\theta_i(x_i)). \tag{4}$$

with $x_i \in \mathcal{P}_i, i = 1...N_{\text{cell}}$ and $V_i^{\text{fix}}(\theta_i(x_i))$ given as:

$$V_i^{\text{fix}}(\theta_i(x_i)) = \begin{cases} \frac{c_1}{(c_2 + \theta_i(x_i))^2}, & \text{if } x_i \in \mathcal{P}_i, \\ 0, & \text{if } x_i \notin \mathcal{P}_i. \end{cases} \tag{5}$$

where c_1 and c_2 are positive parameters representing the strength and effect ranges of repulsive potential.

[2] The function (3) is described in general form, in case that the origin does not belong to the strict interior of the polytope.

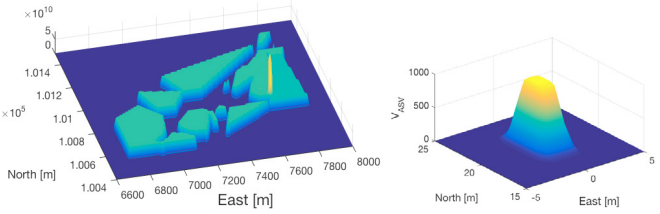

(a) For fixed obstacles (the ground). (b) For the ASV.

Fig. 2. Repulsive potential field.

Fig. 2a illustrates in 3D the total repulsive potential of shore which has high value inside the bounded convex sets and zero outside them. Note that the yellow zone in Fig. 2a denotes the overlap among the bounded polyhedra. The parameters in (5) used for illustration are $c_1 = 0.01$ and $c_2 = 5.10^{-4}$.

2.3 Repulsive potential for the agent

In here we consider N_{mov} moving obstacles which are represented by other agents defined by the dynamical system of an ASV given in (1).

To avoid collision between the ASV and other moving obstacles we construct a repulsive potential for the ASV (which is updated at each step) in order to ensure that the j^{th} moving obstacle cannot enter:

$$V^{\text{mov}}(\mathcal{E}_j(x,y)) = \frac{\lambda_j}{(\gamma_j + \mathcal{E}_j(x,y))^2}. \tag{6}$$

where λ_j and γ_j represent the strength and effect range of ship and $\mathcal{E}_j(x,y)$ is an ellipsoid around the ship which are defined w.r.t. the j^{th} moving obstacle:

$$\mathcal{E}_j(x,y) = \frac{(x_j - x)^2}{r_x^2} + \frac{(y_j - y)^2}{r_y^2}. \tag{7}$$

with (x_j, y_j) the current position of j^{th} moving obstacle, (x,y) is the center of shifted ellipse but also the current position of the ASV and (r_x, r_y) denote the ellipsoid axis and are chosen such that the shape of ASV is covered.

Fig. 2b shows the repulsive potential around a ship. The high value inside the ellipsoid prevents the moving obstacles from colliding with it.

2.4 On-off barrier function

Let us define next an on-off barrier function which will be instrumental in the formulation of the forthcoming motion planning algorithm which activates the constraints only in the field of view of the agent. This function, also called a logistic function (Kyurkchiev and Markov, 2016) was first applied for the study of population growth. It is denoted by:

$$F(x) = \frac{L}{1 + e^{\left(\frac{x - x_o}{\beta^2}\right)}} \approx \begin{cases} 0, \text{ if } x > x_o, \\ \frac{L}{2}, \text{ if } x = x_o, \\ L, \text{ if } x < x_o. \end{cases} \tag{8}$$

where x_o is the x-value of the sigmoid's midpoint, L is the curve's maximum value and β, the steepness of the curve.

Fig. 3 illustrates the on-off barrier function for $L = 1$, $x_o = 100$ and varying β.

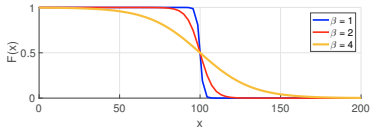

Fig. 3. On-off barrier function as in (8).

Gathering all the elements presented above we will concentrate next on the NMPC implementation for motion planning with collision avoidance. Particular attention is given to the formulation of the cost function through which we penalize the collision avoidance constraints with fixed and moving obstacles.

3 NMPC implementation

A typical approach when using potential field methods is to construct the total potential (attractive and repulsive) and add it into an optimization problem, possibly looking over a prediction horizon. However, this approach is computational cumbersome, especially for difficult applications when the number of fixed and moving obstacles is large. This may lead to infeasible solutions for the optimization problem usually due to local minima. Therefore, this section presents first the combined use of the above constructed repulsive potentials (5), (6) and the on-off barrier function (8) so that the terms of the objective function will be activated only when needed. Next, the NMPC optimization problem and the implementation algorithm are delineated.

3.1 On-off repulsive potential

The safe distance D_s^i of i^{th} cell w.r.t. the agent is calculated by:

$$D_s^i = e\rho_i + \rho_{\text{view}}. \tag{9}$$

where e is an expansion coefficient, ρ_i is the radius of the circle defined from Chebyshev center of the i^{th} forbidden cell, ρ_{view} is the view range of the ship.

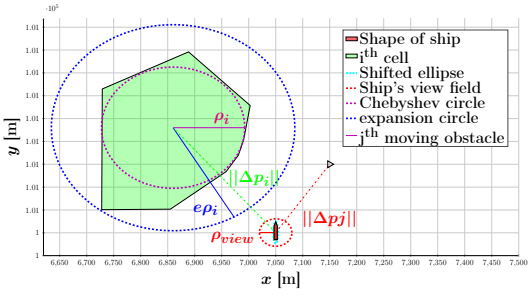

Fig. 4. Description of the safe distance of the ship w.r.t. the i^{th} cell and j^{th} moving obstacle.

Given the set of repulsive potentials, $\mathbb{V}$, as in (5) the agent will take into account the i^{th} repulsive potential $V_i(\theta_i(x_i))$ if and only if the safe distance D_s^i of i^{th} cell w.r.t. the agent is greater than or equal to $\|\Delta p_i\|$.

The on-off barrier function presented in (8) is redefined here for the i^{th} cell as:

$$F_i(x_i) = \frac{L}{1 + e^{\left(\frac{\|\Delta p_i\| - D_s^i}{\beta^2}\right)}} \approx \begin{cases} 0, \text{ if } \|\Delta p_i\| > D_s^i, \\ \frac{L}{2}, \text{ if } \|\Delta p_i\| = D_s^i, \\ L, \text{ if } \|\Delta p_i\| < D_s^i. \end{cases} \tag{10}$$

Consequently, the on-off repulsive potential for the fixed obstacles is described as follows:

$$\Omega_{\text{cell}}(x_i) = \sum_{i=1}^{N_{\text{cell}}} F_i(x_i) V_i^{\text{fix}}(x_i), \tag{11}$$

where $V_i^{\text{fix}}(x_i)$ is given in (5), $F_i(x_i)$ in (10) with $L = 1$. If safe distance D_s^i between agent and i^{th} repulsive potential is guaranteed, i^{th} repulsive potential will be relaxed. If the agent approaches the safe distance D_s^i, the value of i^{th} repulsive potential will be increased to $V_i^{\text{fix}}(x_i)$.

Given the set of moving obstacles, $\mathbb{M}$, the on-off repulsive potential of the agent w.r.t. j^{th} moving obstacle will be taken into account if and only if the view range around this agent is entered by the j^{th} moving obstacle.

Similarly, the on-off barrier function presented in (8) is redefined here for the j^{th} moving obstacle:

$$F_j(x_j) = \frac{L}{1 + e^{\left(\frac{\|\Delta p_j\| - \rho_{\text{view}}}{\beta^2}\right)}} \approx \begin{cases} 0, \text{ if } \|\Delta p_j\| > \rho_{\text{view}}, \\ \frac{L}{2}, \text{ if } \|\Delta p_j\| = \rho_{\text{view}}, \\ L, \text{ if } \|\Delta p_j\| < \rho_{\text{view}}. \end{cases} \tag{12}$$

Hence, the on-off repulsive potential of the agent w.r.t. the moving obstacles is described as follows:

$$\Omega_{\text{mov}}(x_j) = \sum_{j=1}^{N\text{mov}} F_j(x_j) V_j^{\text{mov}}(x_j), \tag{13}$$

where $V_j^{\text{mov}}(x_j)$ is given in (6) and $F_j(x_j)$ in (12) with $L = 1$. If the j^{th} moving obstacle is not in the agent's view range ρ_{view}, the agent's repulsive potential will be relaxed. If the j^{th} moving obstacle is in the agent's view range ρ_{view}, the agent's repulsive potential will be activated.

3.2 NMPC optimization problem

Let us first write in a general form the continuous-time dynamical model of the ship given in detail in (1):

$$\dot{x}(t) = f(x(t), u(t)). \tag{14}$$

with $f : \mathbb{R}^n \times \mathbb{R}^n$, $x \in \mathbb{R}^n$ is the state vector and $u \in \mathbb{R}^m$ represents the control input.

The motion planning optimal control problem is described by (see also Algorithm 1 which describes our proposed approach):

$$\min_{x(.),u(.)} \int_{T_0}^{T_f} L_c(t, x(t), u(t))dt + E(x(T_f)) \tag{15}$$

subject to:

$$x(t_0) = x_0, \tag{16a}$$
$$\dot{x}(t) = f(x(t), u(t)), \tag{16b}$$
$$u_{min} \leq u(t) \leq u_{max}, \tag{16c}$$
$$x_{min} \leq x(t) \leq x_{max}, \ \forall t \in [T_0, T_f]. \tag{16d}$$

with $x_0 \in \mathbb{R}^n$ the initial state of the agent, $x_{min}, x_{max} \in \mathbb{R}^n$ and $u_{min}, u_{max} \in \mathbb{R}^m$. Bounds on the input variations can also be considered.

The stage cost $L_c(.)$ is a composition of multiple objectives with the following expression:

$$L_c(x, u) = \Omega_{\text{cell}}(x_i) + \Omega_{\text{mov}}(x_j) + \|x(t) - x_{ref}(t)\|_Q^2 + \|u(t)\|_R^2. \tag{17}$$

Algorithm 1 NMPC implementation.

Input: Consider model (1), the set of repulsive potentials of the forbidden cells (5) and of the ship (6), the safe distance (9) and the attractive potential (18).

1. Measure the current position $z(k)$ of the ship and predict the position over the prediction horizon T_f.

2. All the information of position of forbidden cells and moving obstacles will be collected by the sensors if they are inside the ship's view range.

3. Solve the NMPC problem:

if $\|\Delta p_i\| > D_s^i$ *and* $\|\Delta p_j\| > \rho_{view}$ **then**

$J = \min_{z,u} \sum_{k=0}^{N-1} (\|z_k - z_k^{ref}\|_Q^2 + \|u_k\|_R^2) + E_N(z_N)$ s.t. (20);

end

if $\|\Delta p_i\| > D_s^i$ *and* $\|\Delta p_j\| \leq \rho_{view}$ **then**

$J_{\text{mov}} = J + \sum_{k=0}^{N-1} (V_j^{\text{mov}}(z_k))$ s.t. (20);

end

if $\|\Delta p_i\| \leq D_s^i$ *and* $\|\Delta p_j\| > \rho_{view}$ **then**

$J_{\text{fix}} = J + \sum_{k=0}^{N-1} (V_i^{\text{fix}}(z_k))$ s.t. (20);

end

if $\|\Delta p_i\| \leq D_s^i$ *and* $\|\Delta p_j\| \leq \rho_{view}$ **then**

$J_{\text{mov}}^{\text{fix}} = J + \sum_{k=0}^{N-1} (V_i^{\text{fix}}(z_k) + V_j^{\text{mov}}(z_k))$ s.t. (20);

end

4. Apply only the first component of the control sequence for system (14).

5. Continue to the next sampling instance, return step 1.

In (17) the term $\|x(t) - x_{ref}(t)\|_Q^2$ represents the attractive potential which has the lowest value at the desired target, x_{ref} (in this particular application, the Trondheim harbor). This term also appears in the terminal cost of (15):

$$E(x(T_f)) = (\|x(T_f) - x_{ref}(T_f)\|_P^2, \tag{18}$$

where Q, R, P are (semi-)positive definite weighting matrices of appropriate dimensions.

Note that the continuous-time optimization problem (15) is non-convex and obtaining the global minimum is not trivial. Therefore, (15) will be discretized using the direct multiple shooting method (Bock and Plitt, 1984). The time horizon $[T_0, T_f]$ is partitioned into N finite subintervals $[t_k, t_{k+1}]$, $k = 0, ..., N-1$, where the state and the control input are defined as explicit optimization variables. Hence, (15) is rewritten in the following discrete-time optimization problem:

$$\min_{z,u} \sum_{k=0}^{N-1} (L_k(z_k, u_k)) + E_N(z_N) \tag{19}$$

subject to:

$$z_0 = x_0, \tag{20a}$$
$$z_{k+1} = \mathcal{F}(t_{k+1}; t_k, z_k, u_k), \quad k = 0, ..., N-1, \tag{20b}$$
$$u_{min} \leq u_k \leq u_{max}, \quad k = 0, ..., N-1, \tag{20c}$$
$$x_{min} \leq z_k \leq x_{max}, \quad k = 0, ..., N. \tag{20d}$$

The function $\mathcal{F}(.)$ as in (20b) is discretized by using the explicit Runge-Kutta integrator of order four (RK4), it shows that step t_{k+1} depends on the previous step t_k. The prediction horizon, T_f, is chosen by multiplying the sampling time T_s and the number of shooting nodes N ($T_f = T_s N$). A control sequence, u_k $(k = 0, ..., N-1)$, over the prediction horizon T_f is obtained by solving (19). Only the first control input over the T_s time-step is applied to the system (14). This optimization problem is implemented by using the interior-point method with Hessian approximation and barrier strategy (ensures a progress towards a local minimum quickly) as in (Zanelli et al., 2017). In here we use FORCES PRO to solve the NMPC optimization problem generating high performance C code (used for real-time implementation) and Matlab executables (used for Matlab simulation).

4 SIMULATION RESULTS

This section continues the application example started at the beginning of the paper. Here we combine all the earlier elements and prove the effectiveness of the proposed algorithm for the safe navigation of a ship in the Trondheim fjord. We use the ASV model (1) with the value of parameters taken from (Pavlov et al., 2009). For simplicity, the Coriolis matrix, wind and wave forces are neglected. We consider constraints on the actuation force $\tau_u \in [-2, 2]$ [N], on the yaw moment $\tau_r \in [-1.5, 1.5]$ [Nm], the surge velocity $u \in [-0.5, 0.5]$ [m/s], the sway velocity $v \in [-0.1, 0.1]$ [m/s] and yaw rate $r \in [-0.2, 0.2]$ [rad/s].

The parameters used in (9) are: the ship's view range $\rho_{\text{view}} = 20$ [m] and the expansion coefficient $e \in [1.2, 1.5]$.

The steepness of the curve used as in (10) and (12) is $\beta = 1.2$. Other parameters of the NMPC optimization problem in (19) are: the prediction horizon is $T_f = 20s$ over $N = 21$ shooting nodes, the simulation time is $1300s$, weighting matrices are $Q = 0.1I_6$, $R = 0.1I_2$, $P = [0.5I_2 \quad 0_2 \quad 0_2; 0_2 \quad I_2 \quad 0_2; 0_2 \quad 0_2 \quad I_2]$.

Finally, the number of cells considered from partitioning the map as in Fig. 1 is $N_{\text{cell}} = 22$.

Simulations are realized by using FORCE PRO via Matlab R2016a on a computer with following configuration: Intel Core i7-4790CPU, 3.60GHz, 8GB RAM.

The travel from Orkanger and Skogn to Trondheim harbor while avoiding collision with static and moving obstacles is considered under the following scenarios:

- *Scenario 1:* use the classical approach where the total potential field appearing in the MPC's cost is active for the entire simulation;
- *Scenario 2:* use Algorithm 1 where the constraints are activated when inside the view range of the agent;
- *Scenario 3:* use Algorithm 1 under the COLGRES rules 8 and 16 given in Section 2.

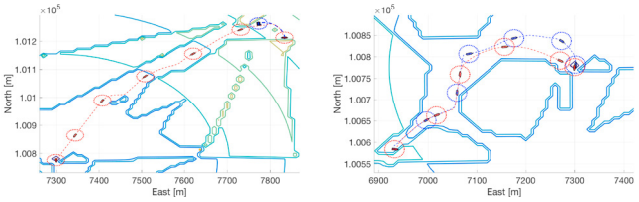

(a) From Skogn to Trondheim. (b) From Orkanger to Trondheim.

Fig. 5. Comparison of trajectories between *Scenario 1&2*.

For *Scenarios 1 and 2* we consider only fixed obstacles represented by the cells given in Fig. 1. For *Scenario 3* moving obstacles are also considered.

Fig. 5a illustrates the actual motion of the agent under *Scenario 1* (blue dashed line) which gets stuck in a local minima because that is a critical area surrounded by many repulsive potentials and their interaction creates a null-potential field. This is the main drawback of the classical approach. This is not the case in *Scenario 2* (red dashed line) which is also represented in Fig. 5a and it can be observed that the ship converges towards the Trondheim harbor without getting stuck in a local minima, this is due to the fact that the number of non-convex constraints (coming from the repulsive potential) are reduced since they are not in the view range of the agent. Notice that the circle around the ship represents its view range.

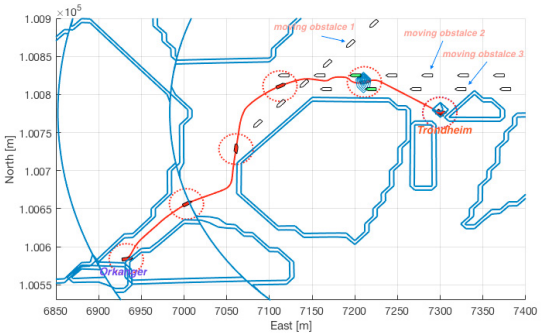

Fig. 6. Ship's collision avoidance complies COLREGS rules 8 and 16 in *Scenario 3*.

Fig. 5b presents a comparison between the agent's trajectory under *Scenario 1* (blue dashed line) and *Scenario 2* (red dashed line). Although the classical approach converges towards Trondheim harbour, evaluation criteria such as smoothness, length of trajectory, number of steps or computation time show that the proposed algorithm is superior to the classical approach. Table 1 gives some details for the two approaches.

Table 1.

Fig. 5b	Scenario 1	Scenario 2
Number of steps	1163	1081
CPU time [s]/step	0.0297	0.0279
Length of trajectory [m]	562.3	512

Fig. 6 shows the effectiveness of algorithms proposed. The trajectory generated following *Scenario 3* can avoid both fixed and three moving obstacles (other ships). Notice that moving obstacles are represented in white colour because they do not belong to the ship's view range. When

moving obstacles are inside the ship's view range, they are presented by green colour and the repulsive potential of the ship is activated in order to implement collision avoidance.

Note that in Fig. 5a, Fig. 5b and Fig. 6, we also illustrate the repulsive and attractive potentials projected in 2D (the repulsive potentials appear around the forbidden region preventing ship's collison with the fixed and moving obstacles and the attractive potential is represented by circles around the destination harbor).

Fig. 7 shows the relative distances between the ship and the three moving obstacles in *Scenario 3*. The relative distances between them depend on strength (λ) and effect range (γ) of the ship's repulsive potential as in (6). In this case, we assume that their safe thresholds are not less than 10 [m], λ and γ are 1000 and 1, respectively.

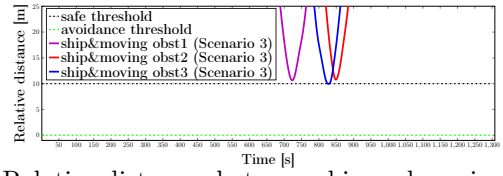

Fig. 7. Relative distances between ship and moving obstalces in *Scenario 3* (Fig. 6).

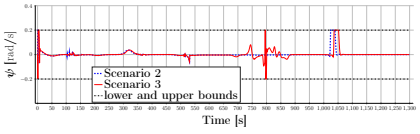

Fig. 8. Yaw rate in *Scenario 2 and 3* (Fig. 5b and 6).

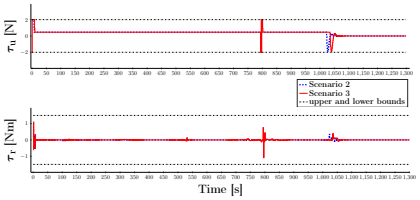

Fig. 9. Control inputs under *Scenario 2 and 3* (of the trajectories presented in Fig. 5b and 6).

Observe in Fig. 8 and Fig. 9, that in the range of 700 to 900 seconds, yaw rate and control input of the proposed algorithm are changed in order to avoid the three moving obstacles that enter the ship's view range obeying rules 8 and 16 of COLREGS.

5 CONCLUSION

This paper proposed an NMPC algorithm for safe navigation of multi-agent systems in an environment with fixed and moving obstacles. The focus was on a real application of motion planning for ships in the Trondheim fjord. Classical non-convex collision avoidance constraints were added in the cost function of an NMPC problem as penalty terms using repulsive potential constructions. These terms were activated only in the view field of the agent. Proof of concept, illustrations, simulations and comparison results over a real benchmark prove the efficiency of the proposed algorithm. Future work will consider other COLREGS rules for this particular application and distributed/decentralized control for multi-agents system. Of further interest is the efficient description of the forbidden areas such that the complexity is reduced and the description is close enough.

Acknowledgements

This work was partly funded by the Research Council of Norway under grant no. 269557.

References

Abichandani, P., Torabi, S., Basu, S., and Benson, H. (2015). Mixed integer nonlinear programming framework for fixed path coordination of multiple underwater vehicles under acoustic communication constraints. *IEEE Journal of Oceanic Engineering*, 40(4), 864–873.

Bock, H.G. and Plitt, K.J. (1984). A multiple shooting algorithm for direct solution of optimal control problems. *IFAC Proceedings Volumes*, 17(2), 1603–1608.

Breivik, M. et al. (2017). Mpc-based mid-level collision avoidance for asvs using nonlinear programming. In *the IEEE Conf. on Control Technol. and Apps.*, 766–772.

Camacho, E.F. and Bordons, C. (2004). Model predictive control. advanced textbooks in control and signal processing. *Springer-Verlag, London*.

Chakravarthy, A. and Ghose, D. (2012). Generalization of the collision cone approach for motion safety in 3-d environments. *Autonomous Robots*, 32(3), 243–266.

Commandant, U. (1999). International regulations for prevention of collisions at sea, 1972 (72 colregs). *US Department of Transportation, US Coast Guard*, 16672.

Dunbabin, M. and Lament, R. (2017). Adaptive receding horizon control for a high-speed autonomous surface vehicle in narrow waterways. In *the IEEE Conference on Control Technology and Applications*, 235–240.

Kyurkchiev, N. and Markov, S. (2016). Approximation of the cut function by some generic logistic functions and applications. *Advances in Applied Sciences*, 1(2), 24–29.

Lee, B.H., Jeon, J.D., and Oh, J.H. (2017). Velocity obstacle based local collision avoidance for a holonomic elliptic robot. *Autonomous Robots*, 41(6), 1347–1363.

Pavlov, A., Nordahl, H., and Breivik, M. (2009). Mpc-based optimal path following for underactuated vessels. *IFAC Proceedings Volumes*, 42(18), 340–345.

Prodan, I., Stoican, F., Olaru, S., and Niculescu, S.I. (2015). *Mixed-integer representations in control design: Mathematical foundations and applications*. Springer.

Rasekhipour, Y., Khajepour, A., Chen, S.K., and Litkouhi, B. (2017). A potential field-based model predictive path-planning controller for autonomous road vehicles. *IEEE Trans. on Intelligent Transp. Systems*, 18(5), 1255–1267.

Shin, J., Kwak, D.J., and Lee, Y.i. (2017). Adaptive path-following control for an unmanned surface vessel using an identified dynamic model. *IEEE/ASME Transactions on Mechatronics*, 22(3), 1143–1153.

Song, R., Liu, Y., and Bucknall, R. (2017). A multi-layered fast marching method for unmanned surface vehicle path planning in a time-variant maritime environment. *Ocean Engineering*, 129, 301–317.

Tran, N.Q.H., Prodan, I., and Lefèvre, L. (2017). Nonlinear optimization for multi-agent motion planning in a multi-obstacle environment. In *21st IEEE Int. Conf. on System Theory, Control and Computing*, 488–493.

Zanelli, A., Domahidi, A., Jerez, J., and Morari, M. (2017). Forces nlp: an efficient implementation of interior-point methods for multistage nonlinear nonconvex programs. *International Journal of Control*, 1–17.